

Studying ELM filaments with Doppler reflectometry in ASDEX Upgrade

E. Trier^{1,2}, P. Hennequin², J.R. Pinzón^{1,3}, M. Hoelzl¹, G.D. Conway¹,
T. Happel¹, G.F. Harrer⁴, F. Mink^{1,3}, F. Orain^{1,5}, E. Wolfrum¹,
the ASDEX Upgrade Team and the EUROfusion MST1 Team*

¹ Max Planck Institute for Plasma Physics, D-85748 Garching, Germany

² LPP, Ecole Polytechnique, CNRS, F-91128 Palaiseau Cedex, France

³ Physik-Department E28, Technische Universität München, 85747 Garching, Germany

⁴ Institute of Applied Physics, TU Wien, Austria, Fusion@ÖAW

⁵ CPHT, Ecole Polytechnique, CNRS, Université Paris-Saclay, 91128 Palaiseau, France

During edge localized modes (ELMs), filaments are expelled from the edge of H-mode plasmas [1]. Shear flows have been shown to be an important ingredient, and are now included in the models [2]. It is therefore essential to investigate experimentally the dynamics of the filaments during an ELM crash. In this contribution, the observation by Doppler reflectometry (DR) of an acceleration, followed by a reversal of the filament velocity during type-I ELMs is reported.

Methodology In ASDEX Upgrade, the Doppler reflectometers are operated in the V (50-75 GHz) and W (75-110 GHz) bands. The received signal has a Doppler-shift in frequency, $f_D = \mathbf{k} \cdot \mathbf{v} / 2\pi$, where \mathbf{k} is the scattering wave-vector defining the spatial scale of the probed density fluctuations and \mathbf{v} their velocity. In H-mode, 'burst-like' events of backscattered signal, with a typical duration of $\sim 10 \mu\text{s}$ are observed [3, 4], either during the inter-ELM phase or the ELM crashes (fig. 1). The Doppler frequency (fig. 1b) is usually well-defined and can be associated to a single event. Some of the strongest of these events can be observed in the inter-ELM phase with other diagnostics (Bolometers, divertor currents), which allows an identification with the filaments. In this study, the filaments and the associated time interval are detected automatically via a threshold in the signal modulus amplitude. The Doppler frequency f_D associated with an event is evaluated in the corresponding time interval. The series of filaments detected during a stationary phase of an H-mode plasma (at the same probing frequency) are ELM-synchronized (the ELM onset t_{ELM} is chosen as the start of the rise in divertor current).

Evolution of the filament motion during ELMs The observed dynamics of the f_D evolution is (fig. 2): an acceleration in the electron direction during the first $\sim 0.2 \text{ms}$ of an ELM, then a reversal in the ion direction for $\sim 1 \text{ms}$, and a recovery for $\Delta t_{ELM} \gtrsim 1 \text{ms}$. This is observed for most of the frequencies probing the pedestal, and for both polarizations. Ray-tracing using the TORBEAM code [5], on ELM-synchronized n_e profiles (fig. 2c) was used to evaluate the

*See author list of "H. Meyer *et al* 2017 Nucl. Fusion **57** 102014"

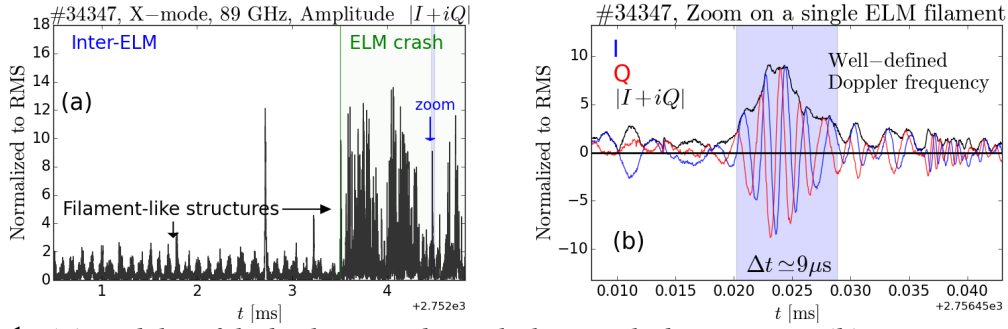


Figure 1: (a) Modulus of the backscattered signal, showing the bursts events. (b) Zoom on a single event during the ELM crash phase, with the I , Q signals output by heterodyne detection.

normalized poloidal radius at the turning point $\langle \rho_{pol} \rangle$ (mapped on a pre-ELM equilibrium) without taking into account the perturbations due to filaments. Above ~ 95 GHz, the turning point is inside the pedestal top $\langle \rho_{pol} \rangle < 0.96$ where the radial electric field is positive. The small value of the pre-ELM Doppler shift (~ 1 km/s) was reported in [4].

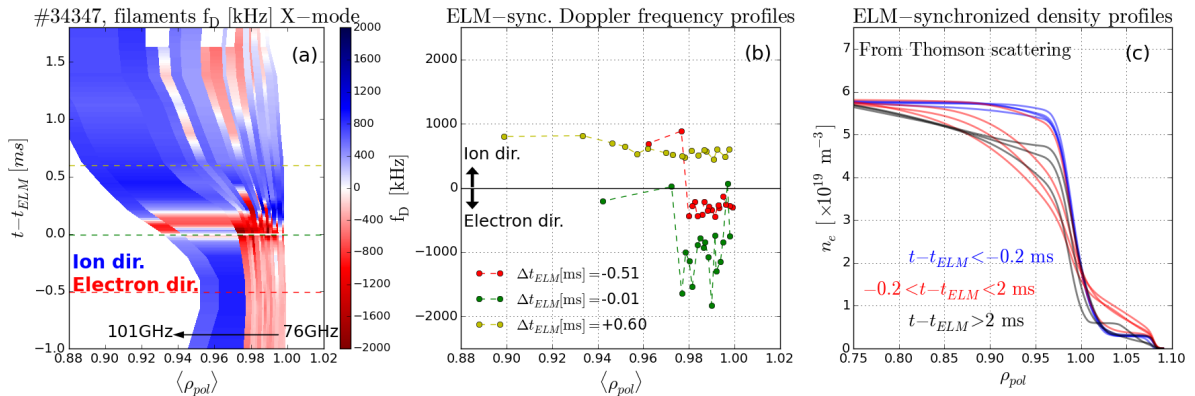


Figure 2: (a) Time evolution of the bin-averaged Doppler frequency f_D of the filaments, as a function of $\langle \rho_{pol} \rangle$ of the turning point. (b) f_D radial profiles. (c) ELM-synchronized density profiles.

Radial or poloidal propagation During an ELM, some filaments are expelled with a radial velocity v_r [1], which could induce a Doppler shift $f_D = k_r v_r / 2\pi$ (originating from the regions where \mathbf{k} has a radial component). This possibility is addressed by comparing measurements with different DR poloidal launching angles, in a way that the perpendicular component of \mathbf{k} at the turning point changes sign. The compared H-mode plasmas with type-I ELMs are #34347 $t = 2 - 4.5$ s (beam launched upwards, angle to the horizontal direction $+4^\circ$), and #34978 $t = 2 - 4.5$ s (downwards, angle -21°). The change of polarity of f_D between these two shots (fig. 3) shows that it is caused by a motion in the perpendicular (rather than radial) direction: indeed, the radial component of the wave dir.-vector along the two probing beams are not of opposite signs.

2D ray tracing using JOREK density maps 2D ray tracing was applied to the n_e fields resulting from a JOREK ELM simulation for a case similar to #34347 [6]. Typical n_e perturba-

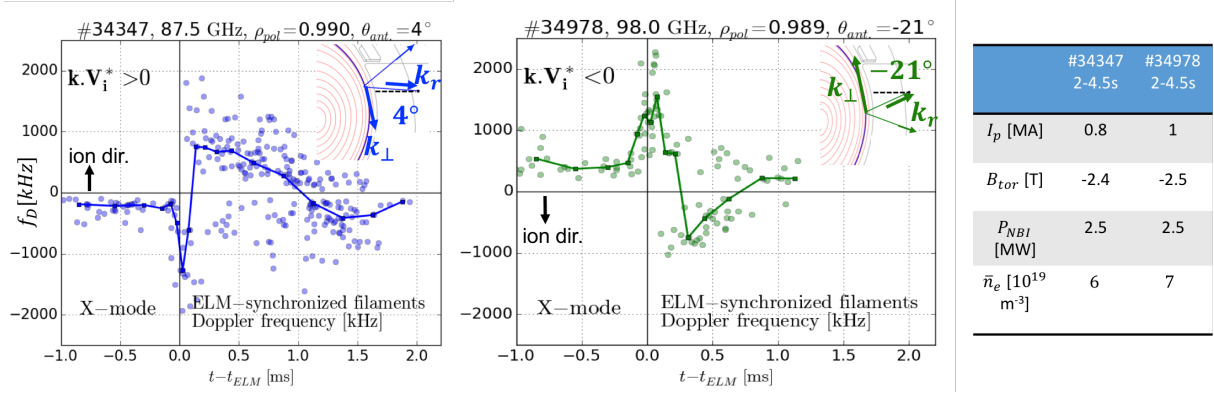


Figure 3: ELM-synchronized Doppler frequency shift of the filament events for two plasmas with reversed direction of the perpendicular component of the wave-vector at the turning point. X-mode polarization is used, at frequencies probing the pedestal ($\rho_{pol} \sim 0.99$).

tions, in the studied time interval $\Delta t_{ELM} = 0.60 - 0.75$ ms, are in the range $\pm 0.5 - 1 \times 10^{19} \text{ m}^{-3}$. The beam is 'modelled' by a series of 5 rays (fig. 4a), with ray equations similar to [7]. The n_e perturbation size in the poloidal direction (typical range is 15 – 40 cm) is larger than the beam dimensions ~ 4 cm. The calculated evolution of ρ_{pol} and the poloidal wave-vector component k_θ at the turning points are represented in figs. 4b and c. It is found that: (i) ρ_{pol} is varying but remains inside the pre-ELM separatrix (ii) k_θ experiences significant variation, with $k_\theta^{max}/k_\theta^{min} \geq 2.2$ for all frequencies (iii) ρ_{pol} and k_θ are almost in quadrature: the minimum of k_θ is reached when ρ_{pol} is close to its mean value. Because the backscattered signal is stronger at lower k (see next section), it results that the localization of the bursts should be well represented by $\langle \rho_{pol} \rangle$, calculated with a n_e profile unperturbed by filaments (like in fig. 2c).

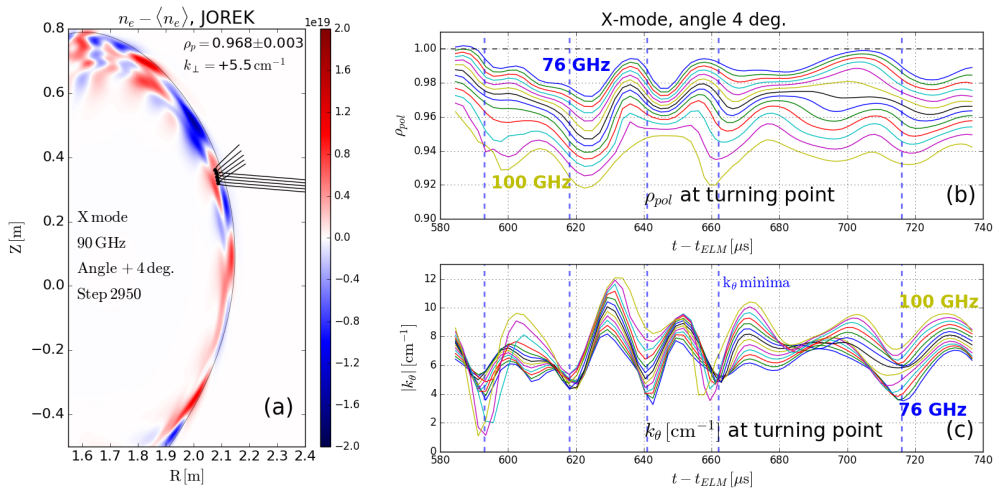


Figure 4: (a) Example of ray-tracing superimposed on ELM n_e perturbations from JOREK calculations. Evolution of averaged quantities at the turning point, for a series of X-mode probing frequencies (76-100 GHz): ρ_{pol} (b) and the poloidal wave-vector k_θ (c). Note the quasi-quadrature between ρ_{pol} and k_θ .

Full wave study in a slab geometry The effect of a n_e perturbation between the antenna and the cut-off is investigated using a full wave code [8]. A perturbation moving in the y -

direction $\delta n_e = \delta n_{e0} \cos(2\pi y/\lambda_b) \exp(-(x-x_b)^2/\Delta x_b^2)$ is added to a density background profile (fig. 5a) with a Gaussian turbulence (fluctuation level: 0.1%). A beam is simulated, with an unperturbed wave-vector $k_y = 6 \text{ cm}^{-1}$ if $\delta n_{e0} = 0$. The perturbation amplitude δn_{e0} is varied from 0 to $2 \times 10^{19} \text{ m}^{-3}$, and its distance to the cut-off from 3 to 1.5 cm. Significant changes of the backscattered signal amplitude are observed (fig. 5b). The main determining parameter is the wave-vector k_y , which can change significantly because the perturbation modulates the beam incidence angle close to the turning point. This results in a stronger signal at low k_{\perp} , qualitatively consistent with the turbulence spectrum shown in fig. 5b.

Conclusion ‘Bursts’ of backscattered signal associated with filaments have been studied during ELMs. The corresponding Doppler shift was found to be due to a motion in the perpendicular direction. After an acceleration in the electron direction for ~ 0.2 ms, rotation in the ion direction is measured during ~ 1 ms. The modulation of the wave-vector due to the n_e perturbations is one possible cause for the increase in signal amplitude, because of the generally stronger turbulence at lower k . The observed qualitative properties of the filament motion during an ELM should be compared with the radial electric field evolution in the future.

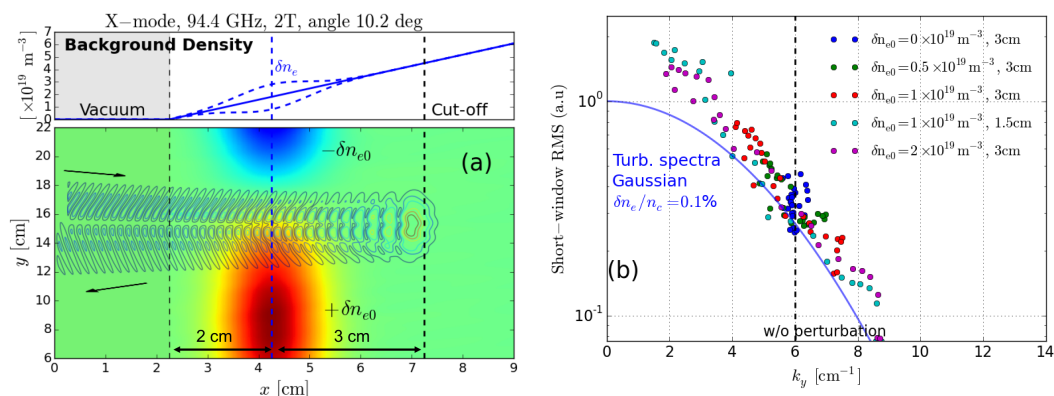


Figure 5: (a) Geometry of the full wave simulation, and background n_e profile. Simulation default parameters are $\Delta x_b = 1 \text{ cm}$, $\lambda_b = 35 \text{ cm}$ (b) RMS values of backscattered amplitude in a moving short-window for several runs, as a function of the k_y wave vector.

References

- [1] A. Kirk et al., Phys. Rev. Lett. **96**, 185001 (2006)
- [2] F. Orain et al., Phys. Plasmas **20**, 102510 (2013)
- [3] V. V. Bulanin et al., Tech. Phys. Lett. **37**, 340 (2011)
- [4] P. Hennequin et al., 44th EPS Conf. on Plasma Physics, P.1.167 (Belfast, Northern Ireland, UK, 2017)
- [5] E. Poli et al., Comput. Phys. Commun. **136** 90 (2001) 026011 (2018)
- [6] M. Hoelzl et al., Contributions to Plasma Physics (accepted)
- [7] C. Honoré et al., Nucl. Fusion **46**, S809 (2006)
- [8] E. Blanco and T. Estrada, Plasma Phys. Control. Fusion **50** 095011 (2008)

Acknowledgements

This work has been carried out within the framework of the EUROfusion Consortium and has received funding from the Euratom research and training programme 2014-2018 under grant agreement No 633053. The views and opinions expressed herein do not necessarily reflect those of the European Commission. G.F. Harrer is a fellow of the Friedrich Schiedel Foundation for Energy Technology.